ACS Sustainable Chemistry & Engineering

Research Article

pubs.acs.org/journal/ascecg

Mo-Doped Cerium Gadolinium Oxide as Environmentally Sustainable Yellow Pigments

Sri Parasara Radhika, Kalarical Janardhanan Sreeram,* and Balachandran Unni Nair

Chemical Laboratory, Central Leather Research Institute, Council of Scientific and Industrial Research, Adyar, Chennai 600 020, India

Supporting Information

ABSTRACT: Mo-doped $Gd_1Ce_{1-x}O_{3.5+Y}$ (where x ranged from 0 to 0.3) oxides were synthesized as inorganic yellow pigments, which are benign and sustainable. The pigments exhibited good yellow color, with the yellowness value using the CIELAB 1976 system being around 39. In comparison to the existing reports on benign yellow pigments, which have been synthesized using high temperature calcination routes, this pigment has been synthesized through a low temperature sol–gel calcination route. The process also provided for a higher degree of size and shape control, leading to a bandgap of 2.82–2.52 eV. Size reduction to the nano level through the process provided a bottom up approach, where the presence of mineralizers enabled higher mass tone (b^* value of around 80) at lower covering thickness. NIR solar reflectance, a measure of the ability of the pigment to contribute to energy savings by reflecting heat generating radiations of sunlight, was as high as 91%. The absence of toxic metal ions coupled with excellent chemical and thermal stabilities makes the developed pigment ideal for coloring plastics meant for children's toys and ceramic surfaces that would come into immediate contact with human skin, such as bathroom tiles.

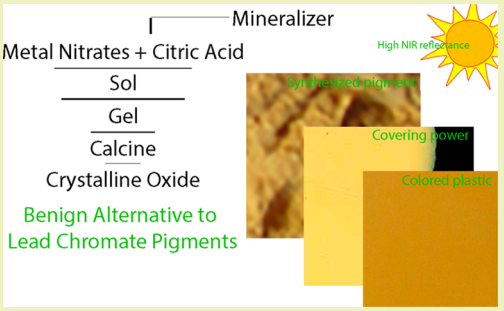

KEYWORDS: *Benign pigments, Doped cerium–molybdenum oxide, Citrate gel, Near-infrared reflectance, CIELAB coordinates, Diffuse reflectance*

INTRODUCTION

Coloring of surfaces with organic or inorganic pigments adds to the aesthetic appeal of the products. Color also enhances multifold the value of the products such as those relating to children, youth, etc. One of the primary concerns of any industry, which relies on the appeal of the colorant employed, is the stability of the color to thermal and chemical deterrents. In this, the inorganic pigments are considered to have an edge over their organic counterparts, though they produce a duller hue than the organics. Yellow has always been an attractive color, with brilliant hues reported with compounds such as $PbCrO_4$, $Pb_2Sb_2O_7$ and CdS. Lead chromates, ever since their inclusion in the substances of very high concern category, are likely to be phased out by 2015, with a predominant replacement by organic/inorganic blends. It has been reported that the organic pigments in combination with titanium dioxide, yellow iron oxide, etc. are ideal replacements for lead chromate. However, for the desired hue and chroma, a higher organic loading is required. The selection of organic pigments is limited by its heat stability, particularly for applications to engineering polymers and chemical resistance—especially when employed on reactive polymers such as polyamides. Other common issues of concern include high oil absorption, migration, bleeding, and warpage.

Though known for their optically pure colors arising from the inner orbital f–f transitions, the development of calcium and lanthanum tantalates, with a perovskite structure as yellow-red pigments has brought renewed interest to these classes of compounds as alternatives to toxic heavy metal ion-based pigments. The electronic configuration of the valence layer of the trivalent lanthanide ions [Xe] 4fn involves the activity of internal f electrons strongly shielded by 5s and 5p electrons. The resulting crystalline field caused by the interaction with neighboring ions is thus very low, and usually the optical spectra of lanthanide compounds present weak and profuse bands. This phenomenon offers a wide scope for the designing of colorants for specific applications. Recently, many researchers including our group have proposed several rare earth-based benign yellow pigments.[1−6]

Among several oxide-based rare earth pigments, cerium oxide has been widely used in recent years because it is a promising material for a number of applications including biosensing and therefore holds a particular place among rare earth oxides.[7−9] The coloring mechanism is based on the charge transfer band from O 2p to Ce 4f in the semiconducting CeO_2.[10] The band gap between the anionic O 2p valence band and the cationic Ce 4f conduction band can be modified by the formation of solid solutions, which introduces an additional electronic level between the valence and the conduction band. As a result, a shift of the charge transfer band is observed. Cerium oxide is a structured oxide that can form extensive solid solutions with a variety of alien cations while retaining the fluorite structure.[11]

Received: February 10, 2014
Revised: March 26, 2014
Published: April 21, 2014

In the CIELAB color coordinates, the L^* represents lightness, a^* represents red/greenness, and b^* represents the yellow/blue character.[12] Mo-doped pigments have a light pale yellow color that nowhere matches that of lead chromate. In order to enhance the b* values, a process of employing multiple dopants has been adopted in this work. The present research work has been undertaken to investigate the effect of molybdenum doping on the color of gadolinium cerium oxide. For this, the lead has come from earlier reports on gadolinium-doped cerium oxides.[13] These oxides have been reported as solid oxide fuel cells.[14,15] Recently, morphological control of gadolinium-doped cerium oxide nanopowders prepared by ultrasonic spray pyrolysis has been reported.[16] Through this paper, we report a facile route employing a combination of classical citrate gel and calcination routes. The citrate gel method allows preparation of highly dispersed mixed oxides. The method involves the formation of a mixed ion citrate, which due to the three-ligand nature of the citrate forms a transparent three-dimensional network upon drying (gel). The pyrolysis of this gel results in homogeneous mixed oxides.

EXPERIMENTAL SECTION

General. Cerium(III) nitrate hexahydrate (99.9% purity), gadolinium(III) nitrate hexahydrate (99.9% purity), ammonium heptamolybdate tetrahydrate (99.98% purity), and citric acid monohydrate (99.9% purity) were sourced from Sigma-Aldrich, U.S.A. All experiments were carried out in triplicate, and the averaged values are reported.

Synthesis. A solution comprising of all the three metal nitrates was prepared, such that the mole composition of the metal ions in solution varied as Gd $(1 - x)$ and Ce xMo, where x ranged from 0 to 0.3 in units of 0.05. The solution was homogenized by stirring, and citric acid (1 M) was added such that the mole ratio of metal to citric acid was 1:1. Stirring was continued for about 10 min, following which the solution was evaporated in a water bath to dryness. A sponge-like solid structure was obtained, during which process a gaseous emission of nitric−nitrous vapors was noticed. The solid material obtained after drying was calcined in an electrically heated furnace to a temperature of 800 °C for a period of 2 h. For this, the furnace was heated to 200 °C at 20 °C/min and subsequently to 800 °C at 5 °C/min. Air-circulating fans placed at the bottom of the chamber enabled heat distribution and effective gradual cooling after the heating period. After cooling to room temperature, the obtained powder was homogenized using a mortar and pestle. Molybdenum-free Ce−Gd was employed as a positive control.

Characterizations. The as-prepared oxides were characterized for size (dynamic light scattering; Malvern, U.K., Zetasizer Nano ZS; water dispersion (100 mg/10 mL); NNLS computation for average size); crystallinity and crystal size (X-ray powder diffraction; Rigaku Multiflex, Ni filtered Cu Kα radiation with λ = 0.154060 nm source and a scintillation counter detector in the 2θ angle range of 10−80° with step size of 0.1°); morphology (scanning electron microscopy, JEOL JSM 5600-LV microscope with an accelerating voltage of 20 kV); and elemental analysis (energy dispersive spectrometer, EDAX). UV−vis diffuse reflectance spectra (UV−vis DRS) were recorded in the absorbance mode at room temperature in the range of 380−780 nm on a Shimadzu (UV-2450) double-beam spectrophotometer equipped with an integrating sphere attachment (ISR 2200) using $BaSO_4$ as the reference. Color analyses were carried out following the CIE recommendations and using the visible spectrum obtained from 380−780 nm (Shimadzu UV-2450 spectrophotometer, UVPC color analysis personal spectroscopy software V3). The color properties are described in terms of the CIE $L^*-a^*-b^*$ system 1976. C^*, which indicates saturation of the color, was calculated using the formula: $C = (a^{*2} + b^{*2})^{1/2}$. The hue angle $H°$ is defined by an angular position in the cylindrical color space; for instance, $H° = 0-35°$ for red and $H° = 35-70°$ orange was also measured. ΔE, the color difference, was computed as

$$\Delta E = \sqrt{(L_1 - L_2)^2 + (a_1 - a_2)^2 + (b_1 - b_2)^2}$$

The absorption/transmission or reflectance of light from the synthesized oxides depends on their electronic structure. Diffuse reflectance studies carried out using an accessory attached to the spectrophotometer play a vital role in the estimation of the band gaps. Reflectance properties of the pigments measured in the region of 700−2500 nm is a relative parameter defined as ratio of flux reflected by the specimen to the flux reflected by a reference surface (in this instance polytetrafluorethylene). The optical band gap was calculated using the Tauc relationship.[17] The Kubelka−Munk (K-M) function converts the diffuse reflectance into an equivalent absorption coefficient.[18] In this relationship, α, the absorption coefficient, is related to reflectance R by the formula

$\alpha = F(R) = (1 - R)^2/2R$. The Tauc relation is then given as $F(R)h\nu = A(h\nu - E_g)^n$. The value of n is 1/2 and 2 for direct and indirect transitions.[19] A plot of $(F(R)h\nu)^2$ versus $h\nu$ and the extrapolation of the linear regions of these plots to $(F(R)h\nu)^2 = 0$ gives the direct band gap values.

NIR solar reflectance (R^*) was calculated in accordance with ASTM standard E891-87. Solar reflectance or the fraction of solar radiation incident at wavelengths between 700−2500 nm is the irradiance weighted average of spectral reflectance, $r(\lambda)$, determined as

$$R^* = \frac{\int_{700}^{2500} r(\lambda) i(\lambda) \mathrm{d}(\lambda)}{\int_{700}^{2500} i(\lambda) \mathrm{d}(\lambda)}$$

where $r(\lambda)$ is the spectral reflectance (Wm^{-2}) obtained from the experiment, and $i(\lambda)$ is the solar spectral irradiance (Wm^{-2} nm^{-1}) obtained from ASTM standard E891-87. Though officially withdrawn, this standard is still in wide use for spectrophotometer and reflectometer calculation of solar reflectance. A vibrating sample magnetometer 4500 was employed to study the magnetic properties of the synthesized pigments with a maximum applied field of 550kA/m at room temperature.

The ability of the pigments to disperse well into long oil alkyd medium and function as a constituent of surface coatings was evaluated by the conventional determination of mass tone. The coloring property of the synthesized yellow pigment was evaluated by incorporating it into a polymer substrate like polymethyl methacrylate (PMMA). A viscous solution of PMMA with the pigment (5 wt %) was prepared using an acralyn cold-curing liquid (Asian Acrylates, India). The thick paste was compressed into a cylindrical disc. Both sides of the pigmented polymer were lapped using a fine grade emery sheet for obtaining a polished surface.

RESULTS AND DISCUSSION

Crystal Structure and Origin of Color. The XRD pattern of the synthesized oxides in the absence and presence of varying mole ratios of molybdenum provided direct clues to the origin of the observed color. Introduction of other elements into the Ce−Gd lattice reduces the lattice size, which in turn influences the band gap and thus the color. It has been reported that by doping with ions with differing ionic radii, the oxygen vacancy and Ce^{3+} concentration can be tuned. The changes in the defect concentration induced by doping can be advantageously employed for various end applications such as catalysis.[20] Similar observations have been made in this work, where the effect of Mo doping on the crystal lattice has been monitored. With ionic radii of 0.0938 nm, the Gd^{3+} ions were small enough to substitute cerium atoms in the crystal lattice, leading to uncharged substitution defects. The formation of these defects is associated with a decrease in the volume of the elementary unit cell. Molybdenum with ionic radii of 0.059 nm

then substitutes into the fluorite structure of CeO_2. This causes an intrinsic strain, leading to a decrease in lattice parameters (a = 5.33 A for 0.35% Mo-doped Ce−Gd oxide, as against a = 5.411 A for CeO_2). The XRD pattern of the oxide (a) (Figure 1) matched with that of the cubic fluorite CeO_2, with the main

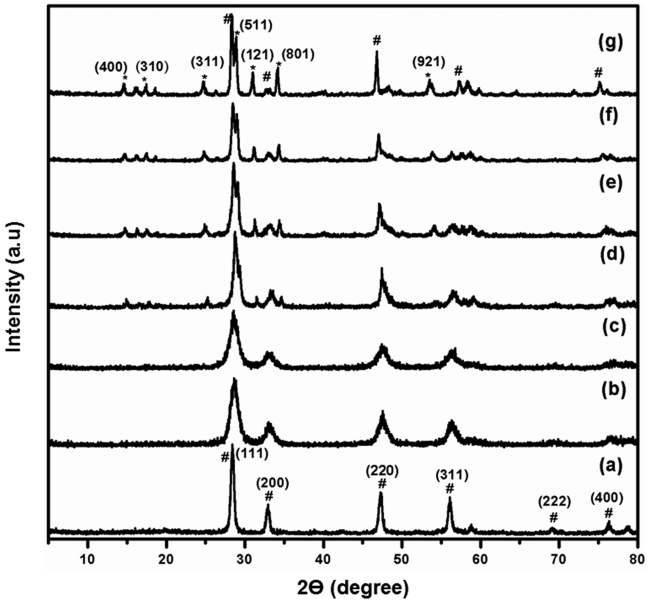

Figure 1. Powder X-ray diffractogram for oxides of Gd−Ce−Mo synthesized from nitrate salts of gadolinium, cerium, and ammonium salt of molybdenum through a sol−gel calcination route (gelation at 100 °C; calcination at 800 °C/2 h). In the figure, the diffractogram for the starting metal ion ratios of Gd:Ce:Mo have been taken into consideration: (a) 1:1:0, (b) 1:0.95:0.05, (c) 1:0.9:0.1, (d) 1:0.85:0.15, (e) 1:0.8:0.20, (f) 1:0.75:0.25, and (g) 1:0.65:0.35.

reflections corresponding to (111), (200), (311), (222), and (400) matching that of JCPDS card no. 34-0394 (cubic fluorite CeO_2, space group Fd_3m). No phases matching that of gadolinium oxide were found, indicating that the Gd ions could have intimately mixed in the CeO_2 lattice. With increasing molybdenum doping (b−g), a broadening of the peaks, corresponding to a smaller crystallite size was observed. At higher concentrations of Mo, peaks corresponding to molybdenum oxide (marked as ∗) appeared alongside CeO_2 phase (#), in agreement with JCPDS card no. 89-6725. The crystallite size calculated using the Debye Scherer formula was found to be in the range of 17−20 nm.

Particles of pigments that are made using these crystals have a size in the region of nanometers to micrometers. The dynamic light scattering technique provides an opportunity to understand the dimensions of particles in terms of diameter, i.e., assuming the particles are all spherical. The intensity average diameter, computed using the standard NNLS technique, was found to decrease from 1079 nm for a Gd−Ce oxide to 731 nm for an oxide with 0.35% Mo doping. The enhanced size could be due to aggregation induced by the dispersion of the particles in water for the DLS measurements. This observation was confirmed from the corresponding SEM image of particles for a 0.35 mol % Mo doping, which indicated a rice-shaped morphology with particle diameters in the range of 240 nm (Figure 2). The EDAX spectra correspondingly showed only peaks of Ce, Mo, and Gd alongside O, indicating that no impurities from starting material could be present. The atomic weight percentage distribution of O, Ce, Gd, and Mo was 79.1, 2.7, 4.6, and 13.6, respectively.

According to the K-M theory, reflectance from a material increases as the particle size decreases; this in turn leads to a reduction in depth of penetration of light and hence absorption. The absorption spectra and diffuse reflectance spectra of the molybdenum-doped oxide is presented in Figure 3, and the corresponding images of the pigment powder is given in Figure S1 of the Supporting Information. For cerium oxide, a strong absorption below 400 nm is attributed to O_{2p}−Ce_{4f} charge transfer transitions. In this particular instance, the absorption observed at 428 nm is attributable to the O_{2p}− Mo_{4d} charge transfer transitions of Mo^{6+}. The band observed at 585 nm is also assigned to the energy levels of $^5D_0$−$^7F_1$ Gd^{3+} transitions. From the color point of view, the absorption of light in the violet−blue region is responsible for the observed yellow color as blue is complementary to yellow. The diffuse reflectance

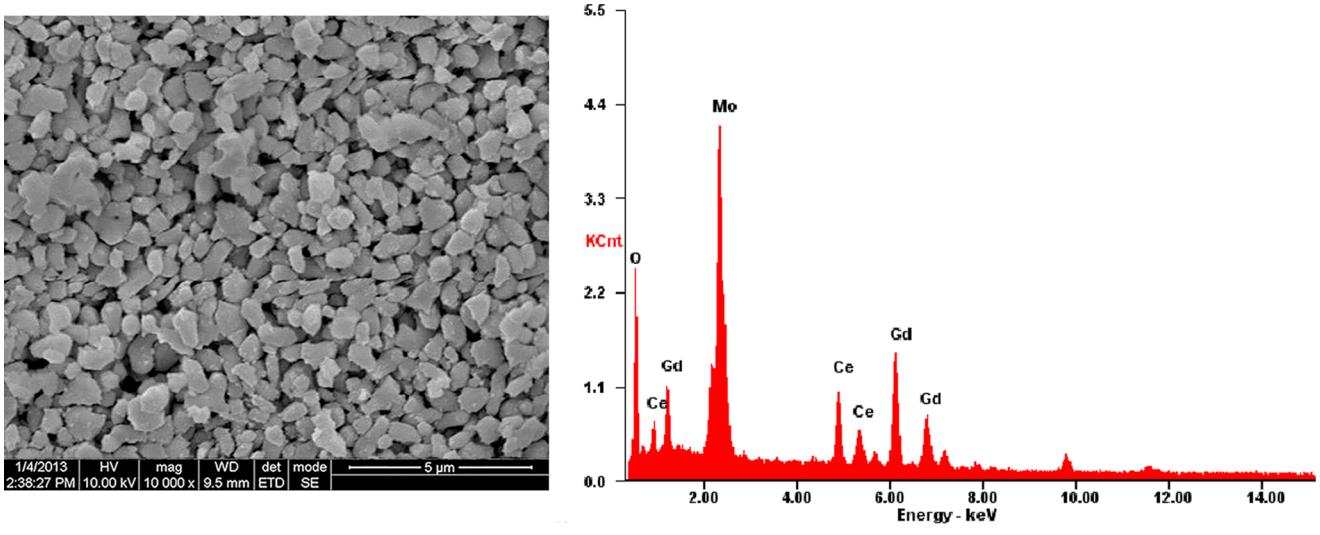

Figure 2. Morphological and elemental analysis for the Ge−Ce−Mo oxide through SEM-EDAX. Oxide was synthesized from nitrate salts of gadolinium and cerium and ammonium salt of molybdenum (1:0.65:0.35) through a sol−gel calcination route (gelation at 100 °C; calcination at 800 °C/2 h).

dx.doi.org/10.1021/sc500085m | ACS Sustainable Chem. Eng. 2014, 2, 1251−1256

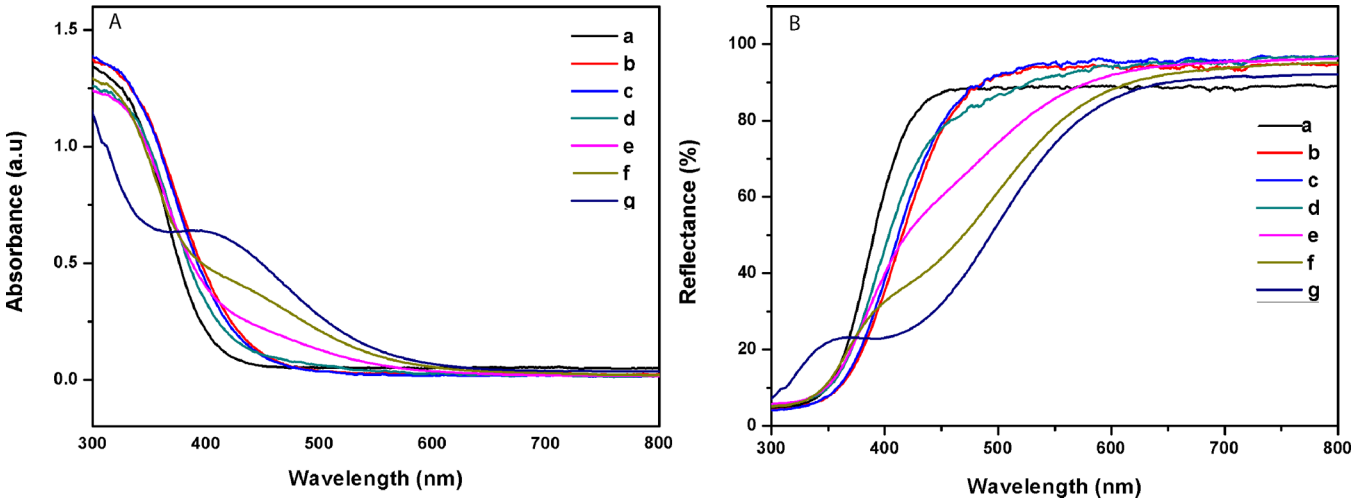

Figure 3. (A) Absorbance spectra. (B) Reflectance spectra for oxides of Gd−Ce−Mo synthesized from nitrate salts of gadolinium and cerium and ammonium salt of molybdenum through a sol−gel calcination route (gelation at 100 °C; calcination at 800 °C/2h). In the figure, spectra for the starting metal ion ratios of Gd:Ce:Mo have been taken into consideration: (a) 1:1:0, (b) 1:0.95:0.05, (c) 1:0.9:0.1, (d) 1:0.85:0.15, (e) 1:0.8:0.20, (f) 1:0.75:0.25, and (g) 1:0.65:0.35.

spectra indicates that that absorption edge shifts from 400 to 585 nm with Mo^{6+} doping on to a Ce^{4+} lattice, with resultant color change from white to dark yellow, alongside a corresponding band gap energy decrease from 2.82 to 2.52 eV. The decrease in the band gap energy could be related to the electronic structure of the Mo^{6+} dopant or to the sp−d exchange interaction between the localized d electrons of Mo^{6+} and band electrons of the Ce−Gd oxide.[21] With increasing doping, a red shift in the charge transfer band is observed. The corresponding chromatic values are recorded in terms of the CIELAB 1976 coordinates. At 0.35 mol % doping of Mo, the b* value was highest, indicating a yellow tone.

Enhanced Near-Infrared Reflectance. Solar energy is made up of approximately 5% UV, 43% visible, and 52% near-infrared radiations.[22] Colored coatings on surfaces exposed to sunlight would then absorb the heat-inducing NIR radiations and heat the interiors, leading to escalting costs for air conditioning. Replacing the conventional pigments with those having high NIR reflectance has been considered as a way forward.[19,22−26] Thus, pigment is considered as "cool" when it is able to reflect the majority of the solar radiation in the 1200−2500 nm region. The NIR solar reflectance spectra and the corresponding solar reflectance value (R^*) is an indication of the cool factor. NIR reflectance from conventional oxide pigments such as cadmium yellow pigment, nickel titanate yellow, and iron oxide yellow has been reported to be 87%, 77%, 70%, respectively. The doping of 0.35 mol % of Mo increases the R^* value to 91% (Figure 4), possibly due to a combination of particle size and phase structure. It is evident that Mo doping resulted in an increase in grain size, i.e., the amount of grain within the same volume decreases and the absorption path of light decreases, with a resultant increase in total reflection.

Magnetic Properties. The magnetization behavior of Mo-doped Ce−Gd oxide pigment was investigated by sweeping the external magnetic field. The field (G) versus moment plot is provided in Figure S2 of the Supporting Information. The presence of Gd in the sample provided for superparamagnetic behavior, as shown from the fact that saturation was never attained even at a very strong applied magnetic field. An M_s value of 13.8 × 10^{-3} emu and coercivity of 399.95 G further confirmed the superparamagnetic behavior. The linear portion in Figure S2 of the Supporting Information can be attributed to the antiferromagnetic phase of MoO_2, while the curved portion may be attributed to the inversion parameter induced by particle size reduction. The presence of nonspherical electron orbitals associated with rare earth metal ions provides for a high anisotropy leading to an increase in domain wall energy and high coercivity.

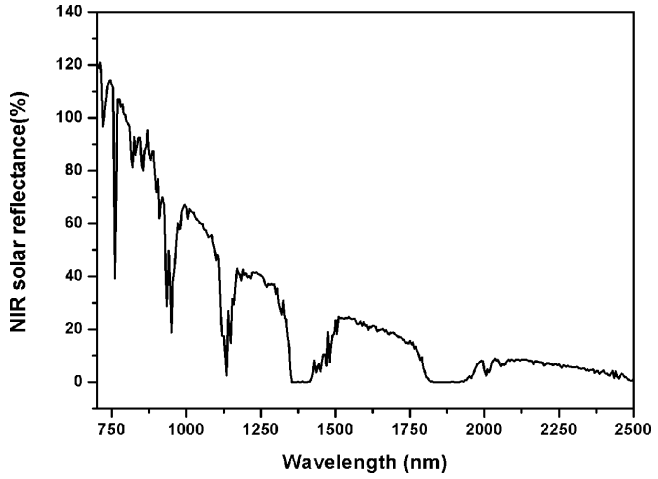

Figure 4. NIR solar reflectance spectra for oxide of Gd−Ce−Mo synthesized from nitrate salts of gadolinium and cerium and ammonium salt of molybdenum (1:0.65:0.35) through a sol−gel calcination route (gelation at 100 °C; calcination at 800 °C/2 h).

Color Performance. The chromatic properties of the synthesized oxides were evaluated using the CIELAB 1976 method and employing a D65 illuminant. The chromatic values described in terms of L* a and b coordinates for Mo doping varying from 0.05 to 0.35% is depicted in Figure 5. For the entire range of doping, the hue angle was around 70 to 105, indicating that the color would remain yellow. The systematic doping of Mo^{6+} (ranging from 0 to 0.35 mol %) for Ce^{4+} in the Ce−Gd oxide results in an increase in the b* value from 3.3 to 39.1, indicating an increasing yellow color. The loss of green

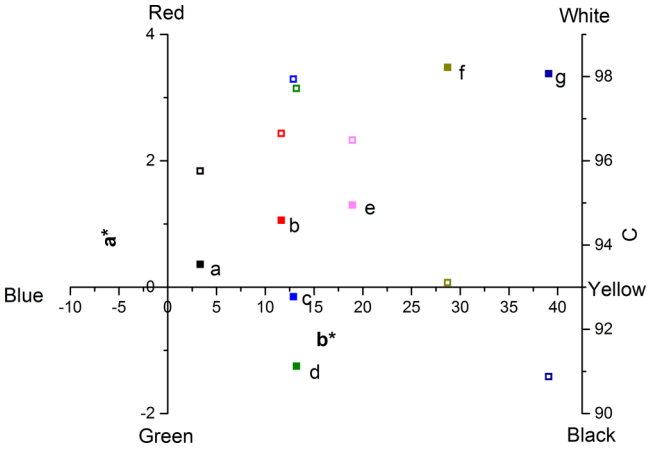

Figure 5. CIELAB 1976 color coordinates for oxides of Gd−Ce−Mo synthesized from nitrate salts of gadolinium and cerium and ammonium salt of molybdenum through a sol−gel calcination route (gelation at 100 °C; calcination at 800 °C/2 h). In the figure, the a^* values have been plotted against the corresponding b^* values on the left axis, and L values on right axis for starting metal ion ratios of Gd:Ce:Mo have been taken into consideration: (a) 1:1:0, (b) 1:0.95:0.05, (c) 1:0.9:0.1, (d) 1:0.85:0.15, (e) 1:0.8:0.20, (f) 1:0.75:0.25, and (g) 1:0.65:0.35.

tinge observed at low concentrations of Mo^{6+} (0.05−0.1 mol %) and gain of red tinge with increasing dopant concentration was also observed. Incidentally, the lightness value remained more or less around 95, indicating that the color did not lighten or darken with doping. This is also reflected in its chroma value (c), which increases from 3.51 to 39.2. As a result, the color changes drastically from green-yellow to red-yellow. The coloring mechanism of the present pigments is essentially based on the charge transfer transition that further intensifies upon doping of Mo^{6+} for Ce^{4+} in the Ce−Gd oxide.

The hue and the color coordinates could be manipulated by addition of mineralizers. Addition of NaF and $NH_4H_2PO_4$ resulted in increase in the b^* value and chroma, corresponding to a red shift of the charge transfer band in the reflectance spectra. Mineralizers such as CaF_2, Na_2CO_3, and H_3BO_3 shifted the hue toward orange-yellow (35−75°) (Table 1). The reflectance spectra in Figure S3 of the Supporting Information indicates a red shift in charge transfer band.

Paint formulations developed using long oil alkyd resins and the pigment with 0.35% Mo had a reasonable covering of the black surface of a black and white checkered board. The color difference (ΔE) in the color coordinates obtained for the coated region on black as against white was taken as a measure of the covering. Computation of the ΔE values from the data reported in Figure S4 of the Supporting Information indicated that at a 300-μm coating thickness the values were 4.7 and 10.4 for an oxide with 0.35% Mo doping and 0% doping, respectively. A lower value of ΔE for the mass tone is an indication of the ability of the oxide to cover the black and white regions effectively well.

Incorporation of 5% of pigment in PMMA was carried out to test the color distribution when molded into plastic. Figure S5 of the Supporting Information provides information on the color of the molded plastic and color coordinates measured at various points. The ΔE value between various points was negligible (<1), indicating the uniform distribution of the pigment in the polymer substrate.

One of the significant aspects that enables an inorganic pigment to stand out from organics is its acid and alkali resistance. As shown in Figure S6 of the Supporting Information, the ΔE value for the pigment after treatment with 2% acid or alkali solution was negligible, indicating their stability to harsh environmental conditions. Bleed resistance was also observed in various solvents with industrial experts giving a visual evaluation value of 10 (on a scale of 0−10, with 0 as worst and 10 as best) for trials in water, mineral turpentine, isopropyl alcohol, methanol, etc. The synthesized oxide with 0.35% Mo doping also met the water-soluble norms (0.24%) laid for pigment for paints (ASTM D50). Light fastness measurements were carried out for a period of 6 h, and no major change in color was observed visually.

In conclusion, the oxide of Ce−Gd−Mo in the mole ratio of 1:0.65:0.35 is an ideal inorganic pigment with good mass tone, solar reflectance, bleed resistance, etc. The oxide could replace conventional toxic pigments such as lead chromate as well.

Table 1. CIELAB 1976 Color Coordinates for Oxides of Gd−Ce−Mo synthesized from Nitrate Salts of Gadolinium and Cerium and Ammonium Salt of Molybdenum (1:0.65:0.35) through a Sol−Gel Calcination Route (gelation at 100 °C; calcination at 800 °C/2 h), in the Presence and Absence of 1% Mineralizer

composition (Gd:Ce:Mo) [1:0.65:0.35]	color coordinates				
	L^*	a^*	b^*	$h°$	c
no mineralizer	90.88	3.38	39.07	85.05	39.22
CaF_2	83.45	10.10	7.22	35.55	12.41
Na_2CO_3	80.78	8.58	11.76	54.13	14.51
H_3BO_3	83.75	10.79	11.23	46.15	15.58
NaF	85.88	−9.02	74.28	96.92	74.83
$NH_4H_2PO_4$	85.16	−7.25	67.22	96.15	67.61

■ ASSOCIATED CONTENT

Supporting Information

Analysis of the performance features of the developed pigment. This material is available free of charge via the Internet at http://pubs.acs.org.

■ AUTHOR INFORMATION

Corresponding Author

*Fax: +91 44 2491 2150. E-mail: kjsreeram@clri.res.in.

Author Contributions

The manuscript was written through contributions of all authors. All authors have given approval to the final version of the manuscript.

Notes

The authors declare no competing financial interest.

■ ACKNOWLEDGMENTS

CSIR-CLRI Communication No. 1061. We thank Miss Sheethu Jose, CSIR-NIIST, Thiruvananthapuram for the NIR Solar reflectance measurements. We appreciate the funding provided by the Department of Science and Technology, GOI, India − WOS Fellowship and Council of Scientific and Industrial Research, New Delhi − XII Plan project SURE.

ABBREVIATIONS

CIELAB = Commission Internationale d'Eclairage 1976 (L^*, a^*, b^*) color space; NIR = near-infrared spectroscopy; EDAX = energy dispersive spectrometry; DRS = diffuse reflectance spectroscopy; ASTM = American Society for Testing and Materials; PMMA = polymethyl methacrylate; XRD = X-ray diffraction; JCPDS = Joint Committee on Powder Diffraction Standards; NNLS = non-negative least squares

REFERENCES

(1) Masui, T.; Honda, T.; Wendusu; Imanaka, N. Novel and environmentally friendly (Bi,Ca,Zn)VO_4 yellow pigments. *Dyes Pigm.* **2013**, *99* (3), 636−641.

(2) Adolfova, L.; Dohnalova, Z.; Sulcova, P. New inorganic pigments based on $SrSnO_3$ doped by V_2O_5. *J. Therm. Anal. Calorim.* **2013**, *113* (1), 161−167.

(3) De la Luz, V.; Prades, M.; Beltran, H.; Cordoncillo, E. Environmental-friendly yellow pigment based on Tb and M (M = Ca or Ba) co-doped Y_2O_3. *J. Eur. Ceram. Soc.* **2013**, *33* (15−16), 3359−3368.

(4) Stranska, L.; Sulcova, P.; Vlcek, M. Synthesis and properties of inorganic pigments based on pyrochlore compounds with different lanthanides. *J. Therm. Anal. Calorim.* **2013**, *113* (1), 127−135.

(5) Sulcova, P.; Stranska, L.; Prokleskova, E. Study of Bi_2O_3 doped by rare-earth element. *J. Therm. Anal. Calorim.* **2013**, *113* (3), 1203−1208.

(6) Zhao, M.; Han, A.; Ye, M.; Wu, T. Preparation and characterization of Fe^{3+} doped $Y_2Ce_2O_7$ pigments with high near-infrared reflectance. *Sol. Energy* **2013**, *97*, 350−355.

(7) Gangopadhyay, S.; Frolov, D. D.; Masunov, A. E.; Seal, S. Structure and properties of cerium oxides in bulk and nanoparticulate forms. *J. Alloys Compd.* **2014**, *584*, 199−208.

(8) Kim, T.; Hyeon, T. Applications of inorganic nanoparticles as therapeutic agents. *Nanotechnology* **2014**, *25* (1), 012001.

(9) Song, Y.; Wei, W.; Qu, X. Colorimetric biosensing using smart materials. *Adv. Mater.* **2011**, *23* (37), 4215−4236.

(10) Patsalas, P.; Logothetidis, S.; Sygellou, L.; Kennou, S., Structure-dependent electronic properties of nanocrystalline cerium oxide films. *Phys. Rev. B* **2003**, *68* (3).

(11) Duran, P.; Capel, F.; Gutierrez, D.; Tartaj, J. I.; Moure, C. Cerium (IV) oxide synthesis and sinterable powders prepared by the polymeric organic complex solution method. *J. Eur. Ceram. Soc.* **2002**, *22* (9−10), 1711−1721.

(12) Corbalan, M.; Millan, M. S.; Yzuel, M. J. Color pattern recognition with CIELAB coordinates. *Optical Engineering* **2002**, *41* (1), 130−138.

(13) Gondolini, A.; Mercadelli, E.; Sanson, A.; Albonetti, S.; Doubova, L.; Boldrini, S. Effects of the microwave heating on the properties of gadolinium-doped cerium oxide prepared by polyol method. *J. Eur. Ceram. Soc.* **2013**, *33* (1), 67−77.

(14) Fabbri, E.; Pergolesi, D.; Traversa, E., Electrode materials: a challenge for the exploitation of protonic solid oxide fuel cells. *Sci. Technol. Adv. Mater.* **2010**, *11* (4).

(15) Stambouli, A. B.; Traversa, E. Solid oxide fuel cells (SOFCs): A review of an environmentally clean and efficient source of energy. *Renewable Sustainable Energy Rev.* **2002**, *6* (5), 433−455.

(16) Halmenschlager, C. M.; Neagu, R.; Rose, L.; Malfatti, C. F.; Bergmann, C. P. Influence of the process parameters on the spray pyrolysis technique, on the synthesis of gadolinium doped-ceria thin film. *Mater. Res. Bull.* **2013**, *48* (2), 207−213.

(17) Wang, S. F.; Gu, F.; Lü, M. K.; Cheng, X. F.; Zou, W. G.; Zhou, G. J.; Wang, S. M.; Zhou, Y. Y. Synthesis and photoluminescence characteristics of Dy^{3+}-doped $ZnAl_2O_4$ nanocrystals via a combustion process. *J. Alloys Compd.* **2005**, *394* (1−2), 255−258.

(18) Ng, J.; Xu, S.; Zhang, X.; Yang, H. Y.; Sun, D. D. Hybridized nanowires and cubes: A novel architecture of a heterojunctioned $TiO_2/SrTiO_3$ thin film for efficient water splitting. *Adv. Funct. Mater.* **2010**, *20* (24), 4287−4294.

(19) Jamal, E.; Kumar, D.; Anantharaman, M. R. On structural, optical and dielectric properties of zinc aluminate nanoparticles. *Bull. Mater. Sci.* **2011**, *34* (2), 251−259.

(20) Suresh, B.; Ranjith, T.; Talgat, I.; Richard, D.; Artëm, E. M.; Alfons, S.; Sudipta, S. Dopant-mediated oxygen vacancy tuning in ceria nanoparticles. *Nanotechnology* **2009**, *20* (8), 085713.

(21) Anand, G. T.; Kennedy, L. J. One-pot microwave combustion synthesis of porous $Zn_{1-x}Cu_xAl_2O_4$ ($0 < x < 0.5$) spinel nanostructures. *J. Nanosci. Nanotechnol.* **2013**, *13* (4), 3096−3103.

(22) Uemoto, K. L.; Sato, N. M. N.; John, V. M. Estimating thermal performance of cool colored paints. *Energy Build.* **2010**, *42* (1), 17−22.

(23) Baneshi, M.; Maruyama, S.; Komiya, A. Comparison between aesthetic and thermal performances of copper oxide and titanium dioxide nano-particulate coatings. *J. Quant. Spectrosc. Radiat. Transfer* **2011**, *112* (7), 1197−1204.

(24) Han, A.; Ye, M.; Zhao, M.; Liao, J.; Wu, T. Crystal structure, chromatic and near-infrared reflective properties of iron doped $YMnO_3$ compounds as colored cool pigments. *Dyes Pigm.* **2013**, *99* (3), 527−530.

(25) Jose, S.; Reddy, M. L. Lanthanum−strontium copper silicates as intense blue inorganic pigments with high near-infrared reflectance. *Dyes Pigm.* **2013**, *98* (3), 540−546.

(26) Wang, J.-L.; Li, Y.-Q.; Byon, Y.-J.; Mei, S.-G.; Zhang, G.-L. Synthesis and characterization of $NiTiO_3$ yellow nano pigment with high solar radiation reflection efficiency. *Powder Technol.* **2013**, *235* (0), 303−306.